Journal of Pharmaceutical Analysis 6 (2016) 235–241

HOSTED BY

Contents lists available at ScienceDirect

Journal of Pharmaceutical Analysis

journal homepage: www.elsevier.com/locate/jpa
www.sciencedirect.com

Original Article

Graphene quantum dot modified glassy carbon electrode for the determination of doxorubicin hydrochloride in human plasma ☆

Nastaran Hashemzadeh [a,b], Mohammad Hasanzadeh [c,d,*], Nasrin Shadjou [e,**], Jamal Eivazi-Ziaei [a], Maryam Khoubnasabjafari [f], Abolghasem Jouyban [d]

[a] Hematology-Oncology Research Center, Tabriz University of Medical Sciences, Tabriz 51664, Iran
[b] Faculty of Pharmacy, Students' Research Committee, Tabriz University of Medical Sciences, Tabriz 51664, Iran
[c] Drug Applied Research Center, Tabriz University of Medical Sciences, Tabriz 51664, Iran
[d] Pharmaceutical Analysis Research Center and Faculty of Pharmacy, Tabriz University of Medical Sciences, Tabriz 51664, Iran
[e] Department of Nanochemistry, Nano Technology Research Center and Faculty of Chemistry Urmia University, Urmia 57154, Iran
[f] Tuberculosis and Lung Disease Research Center, Tabriz University of Medical Sciences, Tabriz 51664, Iran

ARTICLE INFO

Article history:
Received 28 August 2015
Received in revised form
10 March 2016
Accepted 11 March 2016
Available online 11 March 2016

Keywords:
Doxorubicin hydrochloride
Graphene quantum dot
Nanotechnology
Electrochemical sensor

ABSTRACT

Low toxic graphene quantum dot (GQD) was synthesized by pyrolyzing citric acid in alkaline solution and characterized by ultraviolet–visible (UV–vis) spectroscopy, X-ray diffraction (XRD), atomic force microscopy (AFM), spectrofluorimetery and dynamic light scattering (DLS) techniques. GQD was used for electrode modification and electro-oxidation of doxorubicin (DOX) at low potential. A substantial decrease in the overvoltage (−0.56 V) of the DOX oxidation reaction (compared to ordinary electrodes) was observed using GQD as coating of glassy carbon electrode (GCE). Differential pulse voltammetry was used to evaluate the analytical performance of DOX in the presence of phosphate buffer solution (pH 4.0) and good limit of detection was obtained by the proposed sensor. Such ability of GQD to promote the DOX electron-transfer reaction suggests great promise for its application as an electrochemical sensor.

1. Introduction

Graphene quantum dots (GQDs) are nanometer-sized fragments of graphene. GQDs are a kind of 0D material with characteristics derived from both graphene and carbon dots (CDs) [1]. Taking advantages of the electrochemical properties similar to those of graphene, GQDs are widely used as a kind of suitable electrode material, not only in fuel cells [2], supercapacitors [3,4] and photovoltaic cells [5], but also in the field of electrochemical sensors [6,7]. Furthermore, GQDs of tunable sizes, i.e., 2.2 ± 0.3, 2.6 ± 0.2, and 3 ± 0.3 nm, can act as multivalent redox species using cyclic voltammetry (CV) and differential pulse voltammetry (DPV) measurements, and present exciting opportunities for building electrochemical sensors [8]. More recently, GQDs have been used in the area of bioanalysis [6,7,9]. However, their applications in the analytical field have not been explored until now. Due to their unique properties, sensors based on GQDs can achieve a high level of performance.

Toxicity of nanomaterials is one of the major challenges of their applications in science and biotechnology. GQDs have the potential to be remarkably successful in the field of nanobiotechnology due to their excellent opto-electrical properties and extremely low cytotoxicity [10–14]. Currently used quantum dots (CdS, PbS, ZnS, ZnSe, HgTe, Ag_2S, Ag_2Se, $CuInS_2$, $CuInSe_2$, InAs and InP) are composed of toxic metals which may cause problems for their use in biological systems. However, GQDs are increasingly being employed to provide more efficient and less toxic alternatives than currently used quantum dots [15–17]. Studies on human breast cancer have shown that GQDs can easily find their way into the cytoplasm and do not interfere with cell proliferation, which indicates that they are non-toxic materials [15–17].

Furthermore, GQDs expand contact area with the analyte, which increases the electrochemical active surface area to interact with some electroactive analytes. Since geometric surface area is a very important parameter in electrochemistry, modification of different substrates (such as glass, carbon, graphite etc.) by GQDs can increase the rate of electrochemical reaction.

Herein, we developed a highly sensitive electrochemical sensor based on GQD in order to determine low concentration of doxorubicin (DOX) in biological samples. To the best of our knowledge,

☆Peer review under responsibility of Xi'an Jiaotong University.

* Corresponding author at: Drug Applied Research Center, Tabriz University of Medical Sciences, Tabriz 51664, Iran.
** Corresponding author.
E-mail addresses: mhmmd_hasanzadeh@yahoo.com, hasanzadehm@tbzmed.ac.ir (M. Hasanzadeh), Nasrin.shadjou@gmail.com, n.shadjou@urmia.ac.ir (N. Shadjou).

http://dx.doi.org/10.1016/j.jpha.2016.03.003

this is the first report on the determination of DOX based on its direct electrochemical oxidation by graphene quantum dot-glassy carbon electrode (GQD-GCE). Using this system, the detection of low quantities of DOX was realized using differential pulse voltammetry (DPV). The electrode has an ultra-low detection limit during DOX electrooxidation. The electrode for DOX electrooxidation has demonstrated its excellent performance. Furthermore, the proposed sensor (GQD-GCE) was successfully used to detect DOX in human plasma, cerebrospinal fluid, and urine samples.

2. Experimental

2.1. Chemicals and reagents

All chemicals were purchased from Merck (Darmstadt, Germany) and used without further purification. Alumina slurry was purchased from Beuhler (Illinois, USA) and DOX was purchased from Exir Nano Sina Company (Tehran, Iran). All solutions were prepared with deionized water. The stock solution of DOX (0.18 M) was prepared by dissolving an accurate amount of DOX in an appropriate volume of 0.02 M phosphate buffer solution (PBS), pH=4.0 (which was also used as supporting electrolyte), and then stored in the dark place at 4 °C. Additional dilute solutions were prepared daily by accurate dilution just before use. Also the other stock solutions were prepared by dissolving an accurate amount equal to molecular weight of each one in 1000 mL deionized water and then all stored in the dark place at 4 °C.

2.2. Preparation of human plasma samples

Human plasma samples were obtained from the Iranian Blood Transfusion Research Center (Tabriz, Iran) and aliquots were transferred into microtubes and frozen at −4 °C until analysis. Human plasma samples frozen at −4 °C were thawed at room temperature daily and vortexed to ensure homogeneity. After thawing the samples gently, an aliquot of 2 mL of this sample was spiked with DOX, and then acetonitrile with the volume ratio of 2:1 (acetonitrile:plasma) was added to precipitate plasma proteins. The mixture was centrifuged for 10 min at 6000 rpm to separate residues of plasma proteins. Approximately, 2 mL of supernatant was taken and added into supporting electrolyte to reach a total volume of 10 mL.

2.3. Apparatuses and methods

Electrochemical measurements were carried out in a conventional three-electrode cell (from Metrohm) powered by an electrochemical system comprising of AUTOLAB system with PGSTAT302N (Eco Chemie, Utrecht, The Netherlands). The system was run on a PC using NOVA 1.7 software. Saturated Ag/AgCl was used as the reference electrode and the counter electrode (also known as auxiliary electrode), which is usually made of an inert material, platinum. All potentials were measured with respect to the Ag/AgCl which was positioned as close to the working electrode as possible by means of a luggin capillary. GCE (Azar electrode Co., Urmia, Iran) was used as the working electrode. Atomic force microscopy (AFM) experiments were performed in a contact mode by Nanowizard AFM (JPK Instruments AG, Berlin, Germany) mounted on Olympus Invert Microscope IX81 (Olympus Co., Tokyo, Japan). The transmission electron microscope (TEM) images were obtained on Leo 906, Zeiss (Germany). UV–vis spectroscopy was performed by Spectro UV–vis 2502 (Cecil, Cambridge, UK). X-ray powder diffraction (XRD) measurements were performed using Siemens, D500 (Germany). Dynamic light scattering (DLS) was obtained using Malvern 3500 ZS. Spectrofluorimetery test was performed using Jasco, FP-750 (Tokyo, Japan).

3. Results and discussion

3.1. Synthesis of GQDs

An easy bottom-up method was used for the preparation of GQDs. At first, GQDs were synthesized by pyrolyzing citric acid and dispersing the carbonized products into alkaline solutions [18]. Briefly, 2 g of citric acid was put into a beaker and heated to 200 °C by a heating mantle until the citric acid changed to an orange liquid. Then, for preparing GQDs, 100 mL of 10 mg/mL NaOH solution was added into the orange homogenous liquid dropwise with continuous stirring. The obtained GQD solution was stable for at least one month at 4 °C. It is important to point out that the time of synthesis process of GQD was 30 min.

3.2. Characterization of GQDs

Fig. 1A shows the AFM image of synthesized GQDs. The corresponding AFM image shows a single GQD monolayer thin film. As can be seen in Fig. 1B, 90% of the particles represented dark brown color, which was assigned to a size range below 10 nm. Furthermore, the DLS study represented hydrodynamic sizes of GQDs with size distribution of (5 ± 4) nm (Fig. 2A) confirming the AFM results.

The XRD pattern of GQD (Fig. 3A) shows a broad peak centered at around 25θ (0.36 nm), suggesting that the electrochemical process has more active sites along the surfaces of GQD, and the shifted peak to a higher degree, compared with the graphene, indicated that carbonization of citric acid produced graphite structures which had a more compact interlayer spacing than the original graphene.

The UV–vis absorption spectra of GQD (Fig. 2B) illustrate typical absorption of graphene derivatives in the UV region (200–300 nm) with an intensive peak at 340 nm and also a peak at 210 nm. Fig. 3B shows fluorescence spectra of the GQD dispersed in water at room temperature. The GQDs have a broad absorption from 400 to 600 nm. The maximum emission of ~480 nm was obtained with an excitation wavelength of 400 nm. Also when the excitation wavelength changed from 340 to 420 nm, the maximum peaks were constant. This could be explained by the uniformity both in the size and the surface state of those sp^2 clusters contained in GQD which was responsible for the fluorescence of GQD.

3.3. Preparation of bare and GQDs modified electrodes

GCE (2 mm in diameter) was polished to a mirror-like finish with 0.3 and 0.05 μm alumina slurry and then thoroughly rinsed with double distilled water. Then it was successively sonicated in acetone and double distilled water and was allowed to dry at room temperature. A total of 30 μL of GQDs with the concentration of 3 mg/mL was dropped on the surface of electrodes pretreated and allowed to dry for 24 h at 4 °C in a dark place. Then the modified electrodes were rinsed with double distilled water 2 or 3 times and the GQDs modified electrodes were obtained and stored at 4 °C until use.

3.4. Electrochemical behavior

In order to verify the electrocatalytic activity of the modified electrode (GQD-GCE) for determination of DOX, the electrochemical experiments in the presence of DOX were carried out. Fig. 4 shows cyclic voltammograms (CVs) of bare GCE and

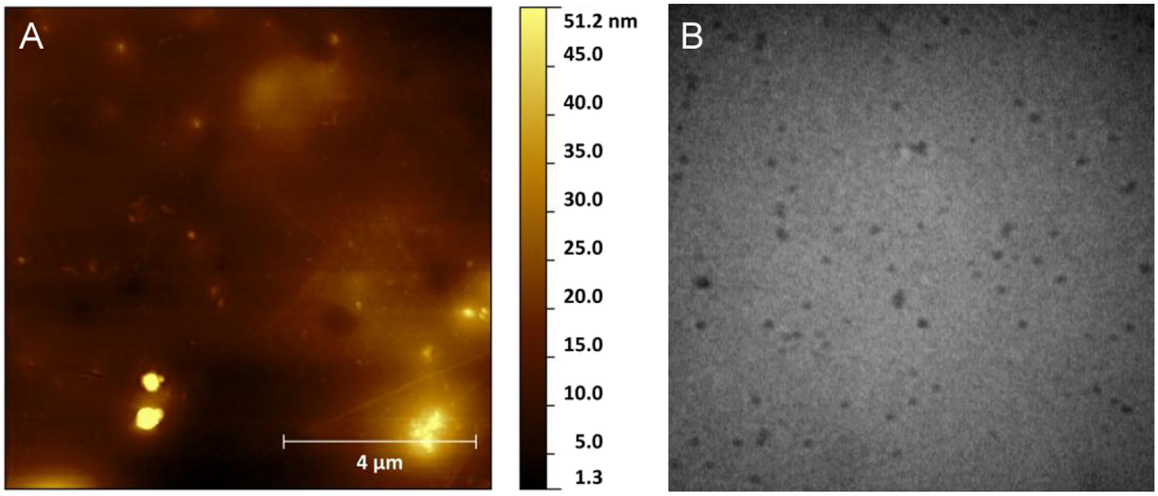

Fig. 1. The AFM (A) and TEM (B) images of GQD.

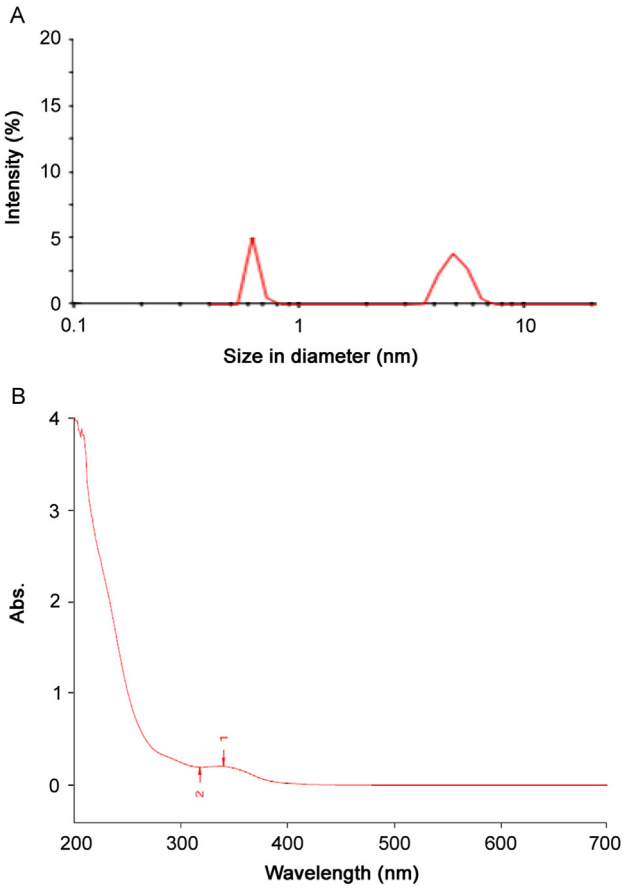

Fig. 2. (A) DLS analysis and (B) UV–vis absorption of GQD.

modified GQD-GCE in the absence and presence of DOX where potential sweep rate of 100 mV/s was employed. CVs show that using GQD-GCE and GCE one pair of redox peaks appeared (Fig. 4). The comparison of recorded CVs in the absence and presence of DOX shows a new anodic peak at −0.56 V on the surface of GQD-GCE. The larger lowering of the overvoltage (−0.56 V) observed in the presence of GQD clearly indicated its essential role in the observed electrocatalytic behavior. These results indicated that GQDs film could accelerate the rate of electron transfer of DOX and had good electrocatalytic activity for redox reaction of DOX. Therefore, GQD is a suitable mediator to shuttle electron between DOX and

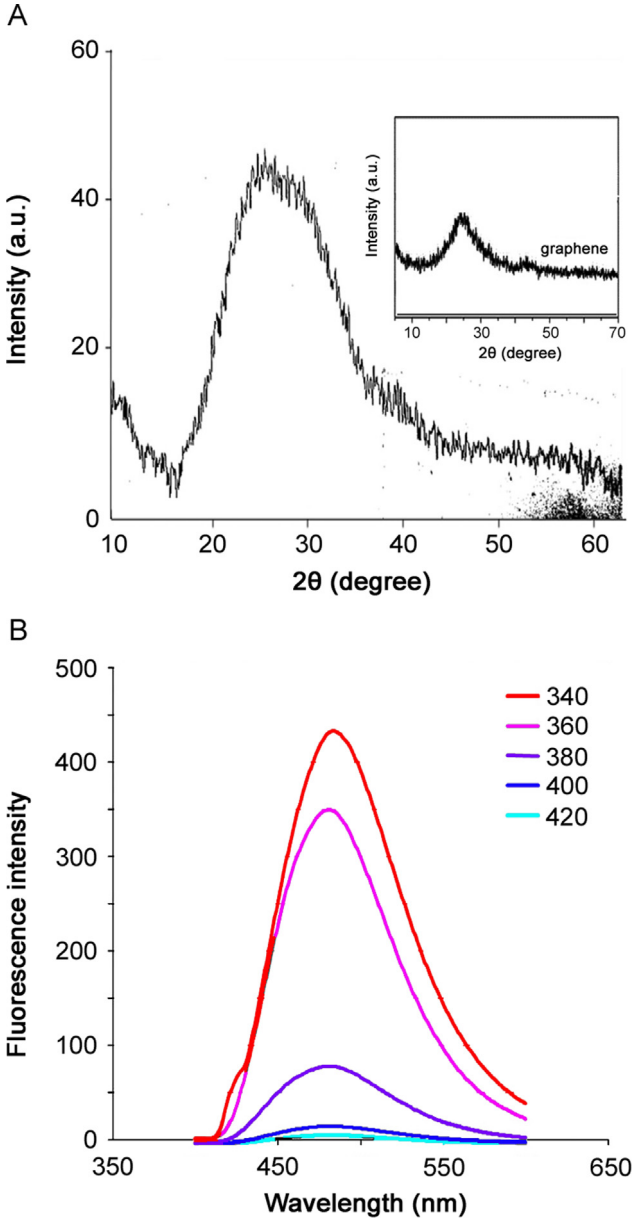

Fig. 3. (A) XRD pattern of GQD and (B) fluorescence spectra of GQD.

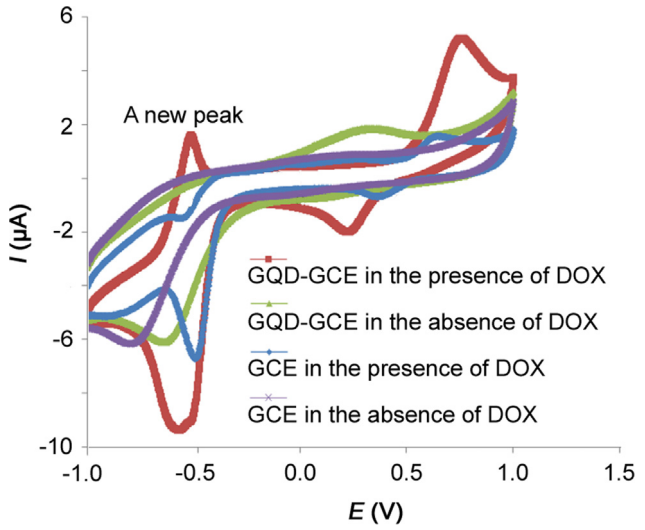

Fig. 4. Cyclic voltammograms of bare GCE and GQD-GCE in the absence and presence of DOX (0.18 mM) in PBS (pH 4.0). Potential sweep rate: 100 mV/s.

working electrode, and facilitate electrochemical regeneration following electron exchange with DOX. This observation is also linked to the high conductivity and inherent ability of GQD. That might be related to the excellent properties of GQD such as high specific surface area and electrical conductivity.

3.5. Effect of modifier amount and pH on the response of GQD-GCE

As shown in Fig. 5A, the first step of modification had a saturation value for the amount of GQDs on the surface of the GCE. The peak current increased with increased amounts of GQDs (20–45 μL). A higher concentration of GQDs showed a decrease in peak current. This is presumably due to the reduction of conductivity of the sensor due to saturation of surface. Consequently, 30 μL of GQDs was chosen as an optimal concentration.

Another important factor influencing the final sensing of the target molecules is pH. In this study, pH values from 3.0 to 7.0 were tested with no substantial differences in sensing peak currents under different pH conditions and pH 4.0 was adopted for sensing (Fig. 5B).

On the other hand, the anodic peak potential of DOX shifted toward negative with an increase in pH (Fig. 5C). These results indicated that the protons took part in their electrode reaction processes. The peak potential (E_p) moved in negative direction with pH rising and they showed such relationship as E_p(DOX)= −0.0625pH +0.473.

The slope of the plot of $Ep_{(Ag/AgCl)}$ versus pH was approximately −0.0625 V (R^2=0.9185). It was therefore deduced that both peaks correspond to irreversible processes involving two electrons and two protons.

This conclusion is in accordance with the known electrochemical reactions of DOX as shown in other investigation. It has been known that DOX can be oxidized via two electrons and two proton processes as shown in Scheme 1.

3.6. Influence of scan rate on the electrooxidation of DOX using GQD-GCE

The effect of the scan rate on DOX electrooxidation was investigated in the range of 2–1000 mV/s using CV (Fig. 6A). A linear relationship was obtained between the peak current and the square root of the scan rate ($v^{1/2}$) in the range of 100–1000 mV/s, which revealed that the oxidation of DOX was an adsorption-

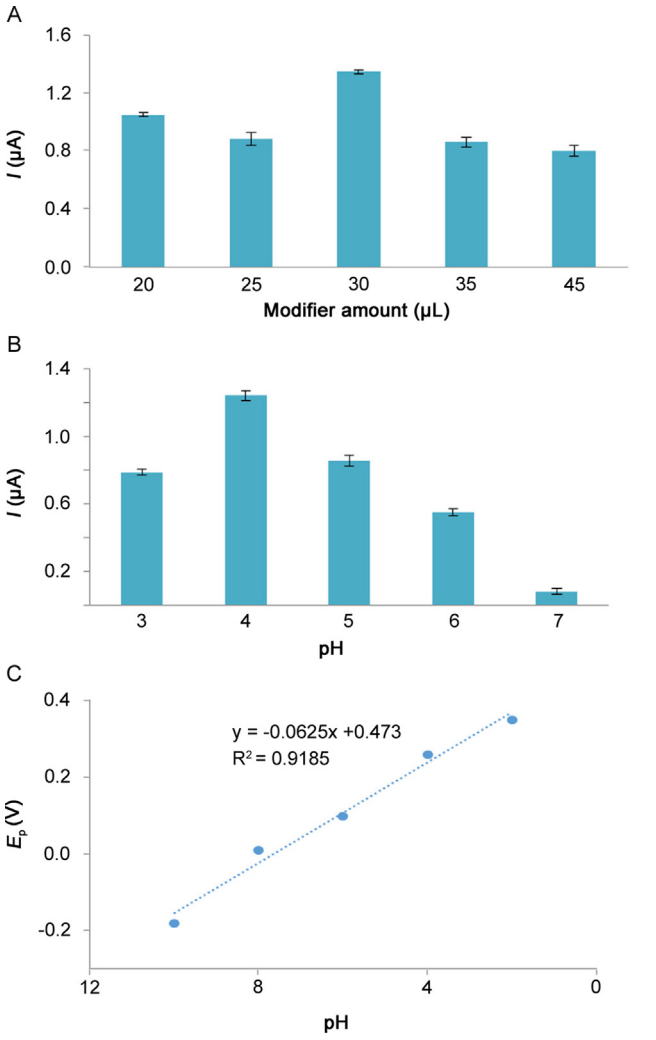

Fig. 5. (A) Variation of peak current versus amounts of GQD (20, 25, 30, 35 and 45 μL) in PBS pH 4.0 (n=3); (B) Influence of PBS pH (3, 4, 5, 6 and 7) on the oxidation peak current; (C) Plot of the Ep versus pH for the GQD-GCE in PBS solution.

controlled step (Fig. 6A). Two approaches widely used to study the reversibility of reactions and to determine whether a reaction is adsorption or diffusion controlled consist of the analyses of dependences: peak current (I_p) vs. $v^{1/2}$ and ln I_p vs. ln v [19–21]. Fig. 6B shows these plots for the oxidation peak of DOX in 0.1 M PBS. For reversible or irreversible systems without kinetic complications, I_p varies linearly with $v^{1/2}$, intercepting the origin. Although the plot of I_p on $v^{1/2}$ presented in Fig. 6B is linear (R^2=0.9904), it does not cross the origin of the axes. This is characteristic for the electrodic process preceded by electrochemical reaction and followed by a homogenous chemical reaction. In the scan rate range from 100 to 1000 mV/s, I_p of DOX electrooxidation depends linearly on square root of the scan rate (v) and is described by the following equation:

I_p=0.0306$v^{1/2}$ [(mV/s)$^{1/2}$ μA]+0.0188 μA (R^2=0.9904).

This dependence crosses the origin (Fig. 6C), which suggests that the electrode process of DOX electrooxidation is controlled by diffusion. On the other hand, dependence of ln I_p on ln v is linear (Fig. 6C) and described by the following equation:

ln I_p={0.4967ln v (V/s)}−0.006 μA (R^2=0.9914).

Its slope is 0.4967, which indicates diffusion-control of the electrode process. A slope close to 0.5 is expected for diffusion-controlled electrode processes and close to 1.0 for adsorption-controlled processes [19–21].

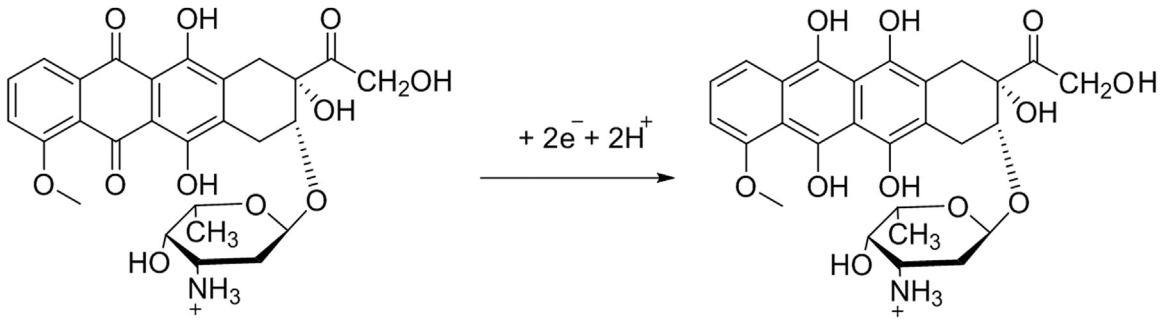

Scheme 1. Tentative mechanism of DOX on GQD-GCE.

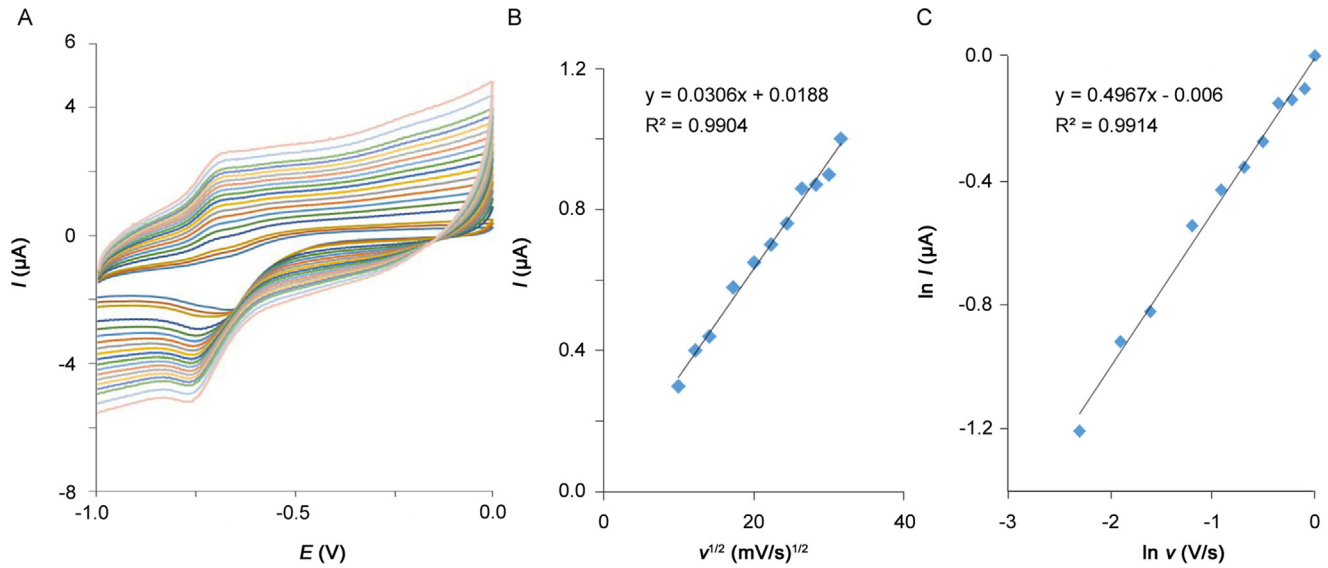

Fig. 6. (A) CVs of GQD-GCE in the presence of 0.1 M PBS (pH 4.0) and 8 μM of DOX in different scan rates (from inner to outer): 20–1000 mV/s, respectively; (B) Dependence of anodic peak current (I_p) on the square root of potential scan rate (ν); (C) Dependence of anodic peak current on the potential scan rate in double logarithm coordinates in the presence of 0.1 M PBS (pH 4.0) at GQD-GCE.

3.7. Analytical application of GQD-GCE on determination of DOX

In order to develop a voltammetric method for DOX determination, we selected the DPV mode, because the peaks are sharper and better defined at lower concentration of DOX than those obtained by CV, with a lower background current, resulting in improved resolution. According to the obtained results, it was possible to apply this technique to the quantitative analysis of DOX. As mentioned previously, the PBS of pH 4.0 was selected as the supporting electrolyte for the quantification of DOX. The maximum peak was observed approximately at −0.56 V for DOX by DPV analysis. As shown in Fig. 7, the peak current increased linearly with the increased concentration of DOX.

The analytical responses of the modified electrode toward the electroanalytical determination of DOX in human plasma samples are listed in Table 1. The proposed method had suitable limit of detection (LOD), wide linear range and good stability compared with those of other methods. This method was checked with respect to linearity (R^2=0.9971), inter-day precision (3.33% RSD), intra-day precision (5.03% RSD) and accuracy.

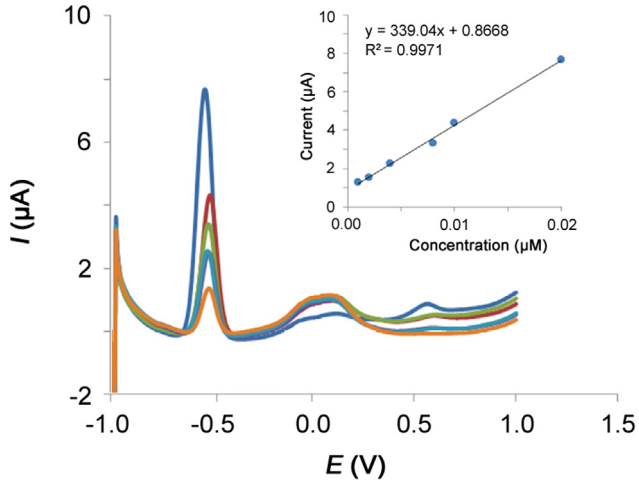

Fig. 7. DPVs of DOX (36×10^{-9}, 18×10^{-9}, 9×10^{-9}, 7×10^{-9}, 45×10^{-10} and 18×10^{-10} M) in PBS pH=4.0 (n=3). Inset: Calibration curve of DOX in spiked human plasma samples.

3.8. Repeatability and long-term stability of the electrode

An extremely attractive feature of the GQD-modified electrodes is their highly stable voltammetric DOX response. The stability of the electrode was determined daily (inter-day) and over one month (intra-day). The obtained RSD% values are less than 1% for inter-day analysis and less than 10% for intra-day determinations up to 10 days. The precision results were not favourable for more than 7 days.

Table 1
Analytical parameters obtained for determination of DOX on GQD-GCE in human plasma.

Analyte	Linear range (μM)	Correlation coefficient (R^2)	Therapeutic range (mg/m^2)	LOD (μM)	LOQ (μM)	Precision (RSD, %)	
						Inter-day	Intra-day
DOX	0.018–3.600	0.9971	60–75	0.016	0.050	3.33	5.03

Table 2
Recovery of DOX in spiked human plasma samples.

Conc. added (μM)	Conc. found (μM)	Recovery (%)	SD ($n=3$)
2.76×10^{-5}	2.48×10^{-5}	90	3.48×10^{-4}
1.84×10^{-5}	1.58×10^{-5}	86	1.10×10^{-3}
9.20×10^{-6}	1.08×10^{-5}	118	8.41×10^{-4}

Table 3
Determination of DOX in patient human plasma samples.

No.	Gender	Age (year)/ body surface (m^2)	Administered dose (mg)	Sampling time	Concentration (μM)
1	Male	27/1.61	35	13 h	3.66×10^{-8}
2	Male	57/1.05	64	5 min	6.79×10^{-8}
3	Male	34/1.84	120	5 min	1.67×10^{-7}
4	Male	18/1.65	120	5 min	1.59×10^{-7}
5	Female	42/1.06	80	5 min	6.27×10^{-8}

3.9. Interference study

In order to evaluate the selectivity of the developed DPV procedure, the effects of various interferences were examined. Considerable interference can be caused by co-existing surface active compounds capable of competing with the analytes of interest for the adsorption site on the electrode surface, resulting in decreased or increased peak height. The competitive co-adsorption interference was evaluated in the presence of various substances usually in biological fluids. For these investigations, different interfering species including glucose, cysteine amino acid, ascorbic acid and uric acid were added at 1 μM concentration. The addition of glucose caused DPV peak current to increase by about 47% in comparison with DOX. Apparently, signal decrease effects were caused by distortion. In contrast, the addition of cysteine amino acid in the drug solution caused the DPV response of the drug to increase by about 13%. Also, the addition of glucose caused DPV peak current to increase by about 10% in comparison with DOX. On the other hand, the addition of uric acid in the drug solution caused the DPV response of the drug to decrease by about 10%. According to the results and the US Food and Drug Administration (US FDA) guideline, only glucose has the obvious change in DOX electroanalytical studies.

3.10. Recovery study

Applicability of the GQD-GCE was examined for the determination of DOX in human plasma samples. The high sensitivity of the sensor allows the determination of DOX in spiked human plasma samples. The recovery of the analytes was measured by spiking DOX into highly diluted plasma samples. The DPVs were recorded after the plasma was spiked with various amounts of DOX within the working concentration range. Recoveries were found in the range of 90%–118% (Table 2).

The efficiency of the electrode was investigated with determination of the DOX concentration in real human plasma samples. These samples were collected after the drug administration. The plasma samples were obtained from patients receiving DOX who had signed consent forms approved by the Ethic Committee, Tabriz University of Medical Sciences, Iran. The results are listed in Table 3.

The comparison of the proposed method with some of other electrochemical reports for the determination of DOX is summarized in Table 4 [22–31]. The analytical parameters of the proposed electrochemical sensor such as LOD, matrix type and linear concentration range are better than or even comparable with the reported data in the literature for electrochemical detection of DOX with different modified electrodes.

Several methods have been reported for determination of DOX in biological matrix, and the results indicate that the modified

Table 4
Comparison of the proposed electrochemical sensor for determination of DOX with some other reports.

Electrode	Method	Linear range(μM)	LOD (μM)	Matrix	Ref.
Silver-amalgam film	SWV[a] and AdSWV[b]	0.0086–0.10283	0.00989	Human urine	[22]
Thiol base sol–gel (TBSol–Gel) modified gold electrode	EIS[c] and CV	4.0–8	1.5	–	[23]
Nano-TiO_2/nafion composite film/GCE	DPV	5.0–2.0	1000	–	[24]
CD-GNs/GCE	DPV	10–0.2	100	–	[25]
CPE[d]	DCV[e] and DPV	–	0.8 (DCV) 0.06 (DPV)	–	[26]
CPE	DPV	0.1–10	0.01	Human urine	[27]
CPE	DPV	–	0.001	–	[27]
CPE	DPV	–	0.00033	–	[29]
Micro-voltammetry	DPV	–	0.001	Chinese hamster ovary cells	[30]
PS/Fe_3O_4-GO-SO_3H/GCE	DPV	0.043–3.5 0.026–3.5 0.86–13.0	0.0049 0.0043 0.014	Plasma Urine Cerebrospinal fluid	[31]
GQD-GCE	DPV	0.018–3.6	0.016	Human plasma	This work

[a] SWV: Cathodic square-wave voltammetry.
[b] AdSWV: adsorptive square wave voltammetry.
[c] EIS: Electrochemical impedance spectroscopy.
[d] CPE: carbon paste electrode.
[e] DCV: Direct current voltammetry.

electrode can be used for detection and determination of DOX without any extraction steps. In most cases, the resulting LODs were significantly more than that of the proposed method. The reported silver-amalgam film [22] presents low LOD value in comparison with these methods. Although dynamic linearity range of the proposed method is not as wide as the others, dynamic linearity range are capable of covering the therapeutic purposes. The proposed electrode is rapid, simple, inexpensive, and sensitive enough for determination of DOX in spiked human plasma.

4. Conclusions

We have illustrated that GQD-GCE offers a stable low-potential voltammetric detection of DOX. The GQD-coating allows a marked decrease in the overvoltage for DOX oxidation. Such electroactivity and stability compare favourably to that observed in other electrode modifier materials. The proposed sensor was used for investigation of DOX in human plasma without a necessity for sample pre-treatment or any time-consuming extraction and evaporation steps prior to the analysis with satisfactory recovery. Additional studies are required for understanding the unique behavior of GQD-modified electrodes towards bioanalysis.

Acknowledgments

This work was a part of a Pharm. D thesis of N. Hashemzadeh. We gratefully acknowledge the partial financial support by the Hematology-Oncology Research Center, Tabriz University of Medical Sciences, under Grants No. 93/5.

References

[1] H. Sun, L. Wu, W. Wei, et al., Recent advances in graphene quantum dots for sensing, Mater. Today 16 (2013) 433–442.
[2] G. He, Y. Song, K. Liu, et al., Oxygen reduction catalyzed by platinum nanoparticles supported on graphene quantum dots, ACS Catal. 3 (2013) 831–838.
[3] W.W. Liu, Y. Feng, X. Yan, et al., Superior micro-supercapacitors based on graphene quantum dots, Adv. Funct. Mater. 23 (2013) 4111–4122.
[4] W.W. Liu, X. Yan, J. Chen, et al., Novel and high-performance asymmetric micro-supercapacitors based on graphene quantum dots and polyaniline nanofibers, Nanoscale 5 (2013) 6053–6062.
[5] V. Gupta, N. Chaudhary, R. Srivastava, et al., Luminscent graphene quantum dots for organic photovoltaic devices, J. Am. Chem. Soc. 133 (2011) 9960–9963.
[6] J. Zhao, G. Chen, L. Zhu, Graphene quantum dots-based platform for the fabrication of electrochemical biosensors, Electrochem. Commun. 13 (2011) 31–33.
[7] H. Razmi, R. Mohammad-Rezaei, Graphene quantum dots as a new substrate for immobilization and direct electrochemistry of glucose oxidase: application to sensitive glucose determination, Biosens. Bioelectron. 41 (2013) 498–504.
[8] D.B. Shinde, V.K. Pillai, Electrochemical resolution of multiple redox events for graphene quantum dots, Angew. Chem. Int. Ed. 52 (2013) 2482–2485.
[9] M. Roushani, Z. Abdi, Novel electrochemical sensor based on graphene quantum dots/riboflavin nanocomposite for the detection of persulfate, Sens. Actuators B 201 (2014) 503–510.
[10] S. Zhu, J. Zhang, C. Qiao, et al., Strongly green-photoluminescent graphene quantum dots for bioimaging applications, Chem. Commun. 47 (2011) 6858–6860.
[11] J. Peng, W. Gao, B.K. Gupta, et al., Graphene quantum dots derived from carbon fibers, Nano Lett. 12 (2012) 844–849.
[12] Y. Dong, C. Chen, X. Zheng, et al., One-step and high yield simultaneous preparation of single- and multi-layer graphene quantum dots from CX-72 carbon black, J. Mater. Chem. 22 (2012) 8764–8766.
[13] M. Zhang, L. Bai, W. Shang, et al., Facile synthesis of water-soluble, highly fluorescent graphene quantum dots as a robust biological label for stem cells, J. Mater. Chem. 22 (2012) 7461–7467.
[14] S. Zhu, J. Zhang, S. Tang, et al., Surface chemistry routes to modulate the photoluminescence of graphene quantum dots: from fluorescence mechanism to up-conversion bioimaging applications, Adv. Funct. Mater. 22 (2012) 4732–4740.
[15] M. Bacon, S.J. Bradley, T.S. Nann, Graphene quantum dots, Part. Part. Syst. Charact. 31 (2014) 415–428.
[16] D. Pan, L. Guo, J. Zhang, et al., Cutting sp^2 clusters in graphene sheets into colloidal graphene quantum dots with strong green fluorescence, J. Mater. Chem. 22 (2012) 3314–3318.
[17] L. Zhang, Y. Xing, N. He, et al., Preparation of graphene quantum dots for bioimaging application, J. Nanosci. Nanotechnol. 12 (2012) 2924–2928.
[18] M. Amjadi, J.L. Manzoori, T. Hallaj, Chemiluminescence of graphene quantum dots and its application to the determination of uric acid, J. Lumin. 153 (2014) 73–78.
[19] J. Xu, F. Shang, J.H. Luong, et al., Direct electrochemistry of horseradish peroxidase immobilized on a monolayer modified nanowire array electrode, Biosens. Bioelectron. 25 (2010) 1313–1318.
[20] P. Kissinger, W.R. Heineman, Laboratory Techniques in Electroanalytical Chemistry, 2nd ed., CRC Press, New York, 1996, pp. 224.
[21] A.J. Bard, L.R. Faulkner, Electrochemical Methods: Fundamentals and Applications, in: 2nd ed., John Wiley & Sons, New York, 2001, pp. 236 503, 709.
[22] Q. Yan, W. Priebe, J.B. Chaires, et al., Interaction of doxorubicin and its derivatives with DNA: elucidation by resonance Raman and surface-enhanced resonance Raman spectroscopy, Biospectroscopy 3 (1997) 307–316.
[23] K. Hirano, T. Nagae, T. Adachi, et al., Determination of adriamycin by enzyme immunoassay, J. Pharm. Dyn. 6 (1983) 588–594.
[24] B. Rezaei, N. Askarpour, A.A. Ensafi, A novel sensitive doxorubicin impedimetric immunosensor based on a specific monoclonal antibody-gold nanoparticle-sol-gel modified electrode, Talanta 119 (2014) 164–169.
[25] J.G. Guan, Y.Q. Miao, Q.J. Zhang, Impedimetric biosensors, J. Biosci. Bioeng. 97 (2004) 219–226.
[26] J.J. Gooding, C. Wasiowych, D. Barnett, et al., Electrochemical modulation of antigen-antibody binding, Biosens. Bioelectron. 20 (2004) 260–268.
[27] Y. Guo, Y. Chen, Q. Zhao, et al., Electrochemical sensor for ultrasensitive determination of doxorubicin and methotrexate based on cyclodextrin-graphene hybrid nanosheets, Electroanalysis 23 (2011) 2400–2407.
[28] Z. Jemelková, J. Zima, J. Barek, et al., Voltammetric and amperometric determination of doxorubicin using carbon paste electrodes, Chem. Commun. 74 (2009) 1503–1515.
[29] E.N. Chaney, R.P. Baldwin, Preconcentration of phenanthrenequinone-like compounds for electrochemical determination at a carbon paste electrode via spontaneous adsorption, Anal. Chem. 54 (1982) 2556–2560.
[30] R.P. Baldwin, D. Packett, T.M. Woodcock, Electrochemical behavior of adriamycin at carbon paste electrodes, Anal. Chem. 53 (1981) 540–542.
[31] J. Soleymani, M. Hasanzadeh, N. Shadjou, et al., A new kinetic–mechanistic approach to elucidate electrooxidation of doxorubicin hydrochloride in unprocessed human fluids using magnetic graphene based nanocomposite modified glassy carbon electrode, Mater. Sci. Eng. C 61 (2016) 638–650.